Solid Electrolytes

DOI: 10.1002/ange.200903598

High Proton Conductivity in Anodic ZrO_2/WO_3 Nanofilms**

*Damian Kowalski, Yoshitaka Aoki, and Hiroki Habazaki**

Anodization of the valve metals Al, Ti, Zr, Nb, Hf, Ta, and W leads to formation of barrier-type (compact) or self-organized porous-type anodic oxide films, depending on the electrolytes used. The oxide films formed are dielectrics or semiconductors with useful properties that make them of great interest for many applications, including solid electrolytic capacitors, solar cells, photocatalysis, electrochromic devices, and self-cleaning materials.[1–2] Here we report the first example of an anodic oxide with high proton conductivity below 200 °C. Proton-conducting thin films are promising electrolytes for solid-oxide fuel cells that operate at intermediate temperatures (100–400 °C) and other electrochemical devices.[3] Intermediate-temperature fuel cells have several advantages over polymer electrolyte fuel cells, which operate below 100 °C, under fully hydrated conditions.[4] The former type allows the use of nonprecious-metal electrocatalysts[5] and hydrocarbon fuels[6] and facilitates simpler module assembly by means of anhydrous proton conductors.

Inorganic solid acids such as $CsHSO_4$, $Rb_3H(SeO_4)_2$, and CsH_2PO_4 exhibit sufficient proton conductivities fuel-cell operation, but their poor processability and low stability limit their practical application.[7] ZrO_2/WO_3 is a very attractive acid catalyst that displays high catalytic activity and stability in demanding reactions that require strong Brønsted acidity.[8] The acid strength of this material has been reported to be $H_o \leq -14.5$ and is comparable with that of fully anhydrous hydrofluoric acid.[9] The proton-transport properties of this material are therefore of great interest.

For practical use of a solid electrolyte in fuel-cell technology, the area-specific resistivity (ASR) of the electrolyte should be below 0.2 $\Omega\,cm^2$.[10] To obtain a sufficiently low ASR value at temperatures below 400 °C, one approach is reducing the thickness of the solid electrolyte to the nanometer scale. Shim et al. reported atomic-layer deposition of yttria-stabilized zirconia nanofilms of 60 nm thickness, which showed high ion conductivity as an electrolyte for solid-oxide fuel cells operated at and below 350 °C.[11] The high proton conductivity of nanofilms below 400 °C has also been reported for amorphous metallosilicate[12] and zirconium pyrophosphate[13] nanofilms prepared by a layer-by-layer sol–gel process. Native protons in these amorphous nanofilms contribute to efficient ionic conduction even in a dry atmosphere.

Anodic oxide films formed on valve metals usually contain hydrogen species.[14] It is likely that high proton conductivity occurs in anodic oxide if the oxide is strongly acidic. In addition, the anodizing process is suitable for fabricating nanofilms of a desired thickness, since the thickness of barrier-type anodic oxide films changes linearly with the formation voltage. In this work, we prepared ZrO_2/WO_3 nanofilms by anodizing magnetron-sputtered Zr/50 atom % W alloy films with flat surfaces. The obtained anodic oxide films showed high proton conductivity even below 100 °C in a dry atmosphere; enhanced conductivity was observed when the thickness of the anodic film was reduced to less than 120 nm. An ASR value of 0.2 $\Omega\,cm^2$ was achieved at a temperature as low as 100 °C for the 60 nm-thick oxide film.

The anodic ZrO_2/WO_3 films were prepared by anodizing sputter-deposited Zr/50 atom % W alloy at several formation voltages in 0.1 mol dm^{-3} phosphoric acid electrolyte. The thicknesses of the anodic oxide films varied from 40 to 180 nm. Figure 1 shows a transmission electron micrograph of an ultramicrotomed section of the Zr/50 atom % W alloy anodized at 50 V. The anodic film, 100 nm thick, with flat and parallel metal/film and film/electrolyte interfaces, developed on the alloy film, which can be seen at the bottom of the micrograph. The anodic film is amorphous and consists of three layers. The outer layer, which accounts for about 12 % of the film thickness, is composed of ZrO_2, essentially free from tungsten species, whereas the remaining film region contains both zirconium and tungsten species. In addition, phosphate anions are incorporated in the outer half of the film thickness, similar to the well-studied amorphous anodic oxide films formed on niobium[15] and tantalum[16] in phosphoric acid. The depth distribution of each element was confirmed by depth-profile analysis with glow-discharge

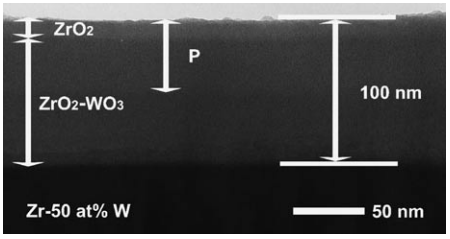

Figure 1. Transmission electron micrograph of an ultramicrotomed section of the sputter-deposited Zr/50 atom % W alloy film anodized at 50 V with current decay for 1.8 ks in 0.1 mol dm^{-3} phosphoric acid electrolyte at 20 °C. The film consists of an 88 nm-thick ZrO_2/WO_3 inner layer and a 12 nm-thick ZrO_2 outer layer (free of W species). Phosphorus species are incorporated from the anodizing electrolyte into 50 % of the anodic oxide film.

[*] Dr. D. Kowalski, Dr. Y. Aoki, Prof. H. Habazaki
Graduate School of Engineering, Hokkaido University
Kita-13, Nishi-8, Kita-ku, Sapporo, 060-8628 (Japan)
Fax: (+81) 11-706-6575
E-mail: habazaki@eng.hokudai.ac.jp

[**] This work was financially supported in part by Global Center of Excellence (GCOE) Program "Catalysis as the basis for Innovation in Materials Science" from Ministry of Education, Culture, Sports, Science and Technology (MEXT) of Japan.

Supporting information for this article is available on the WWW under http://dx.doi.org/10.1002/anie.200903598.

optical emission spectroscopy (GDOES) and Rutherford backscattering spectroscopy (RBS; see the Supporting Information, Figures S1a and S1b).

After depositing an Au button electrode on the anodic oxide film, the resistivity across the anodic film was determined by ac impedance spectroscopy. Efficient proton conductivity was observed after thermal treatment at 200 °C in dry and humidified atmospheres. Thus, conductivity measurements were typically carried out after activation treatment at 200 °C in a dry argon atmosphere for 3.6 ks. Long-term exposure in a humidified ($p_{H_2O} = 0.023$ atm) atmosphere at room temperature also activated the ionic conductivity. Nyquist plots of the activated specimens revealed a small semicircle in the high-frequency region and a spike in the low-frequency region, typical of ionic conductors with blocking electrodes (Figure 2a).[17] The high-frequency semicircle is associated with ionic conduction in the oxide film and becomes smaller with increasing temperature. The low-frequency spike is related to charge buildup at the film/electrode interface.

The conducting ionic species in the present ZrO_2/WO_3 anodic films below 200 °C must be protons. To verify this, the isotope effect was examined. Figure 2c shows the conductivity as a function of exposure time in argon atmospheres containing H_2O or D_2O at a partial pressure of 0.023 atm. During the experiment, Ar/H_2O was exchanged with Ar/D_2O and vice versa every 24 or 48 h. The ASR value thereby increases reversibly in the Ar/D_2O atmosphere owing to the isotope effect for proton conduction.[18] Though the magnitude of the isotope effect of 1.15 is slightly smaller than the value expected for classical proton-hopping migration,[19] protons can be concluded to be among the main charge carriers in the anodic ZrO_2/WO_3 film. A nonclassical isotope effect has also been reported for intermediate-temperature proton conductors like SnP_2O_7 and high-temperature perovskite oxides.[19,20] The ion conductivity of the anodic oxide films measured in a dry Ar atmosphere was not influenced by addition of H_2, O_2, and H_2O to the atmosphere, and this suggests that native protons in the anodic oxide film predominantly contribute to the ionic conduction.

The temperature dependence of the proton conductivity σ of the anodic oxide films with various thicknesses in a dry Ar atmosphere is plotted in Figure 2b. Interestingly, a marked influence of film thickness on proton conductivity was found. The conductivity increases with decreasing film thickness, particularly below 120 nm. This thickness dependence is clearly seen in Figure 3a, in which σ at 50 and 100 °C is plotted as a function of film thickness. The change in conductivity is notable in the thickness range of 80–100 nm at both temperatures. The conductivity is enhanced by 1.3 orders of magnitude on reducing the thickness from 120 to 60 nm. In Figure 2b, the proton conductivity exhibits Arrhenius behavior for all film thicknesses in the investigated temperature range, and the activation energy E_a changes from 27 ± 1.4 kJ mol^{-1} for the 40 nm-thick film to 50 ± 0.3 kJ mol^{-1} for the 180 nm-thick film.

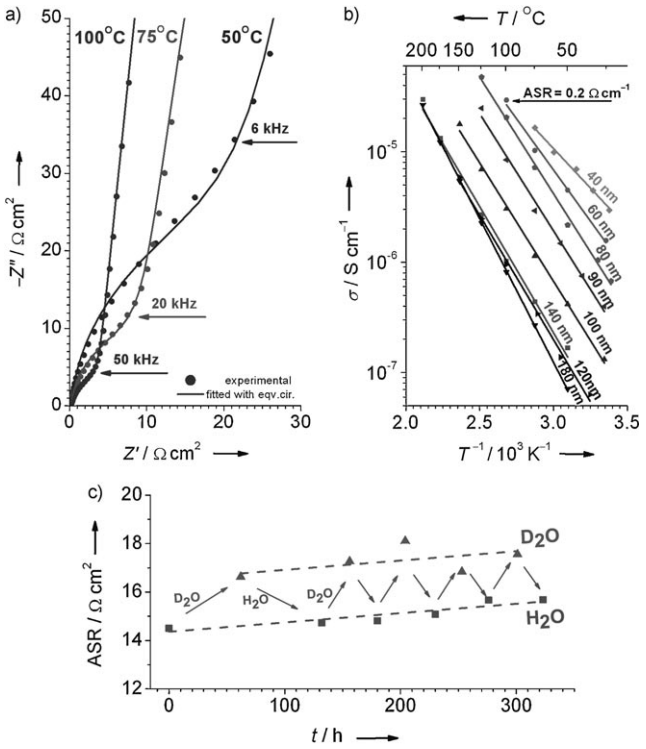

Figure 2. Alternating-current impedance spectroscopy data for Zr–W/anodic oxide/Au system. a) Nyquist plots measured in dry Ar atmosphere at 50, 75, and 100 °C for 100 nm-thick anodic oxide; specimen activated by heat treatment in dry Ar atmosphere. b) Arrhenius plots of proton conductivity, σ, for Zr–W/anodic oxide/Au as a function of film thickness in dry Ar atmosphere; specimen activated by heat treatment in dry Ar atmosphere. c) Isotope-effect study by repeated exposure of Zr–W/anodic oxide/Au system to Ar/H_2O and Ar/D_2O atmospheres ($p_{H_2O} = p_{D_2O} = 0.023$ atm) at 25 °C for 100 nm-thick anodic oxide; specimen activated by long-term exposure in humidified Ar atmosphere.

There are two possible explanations for the enhancement of proton conductivity by reduction of film thickness: 1) the finite-size effect in percolative conduction and 2) the barrier

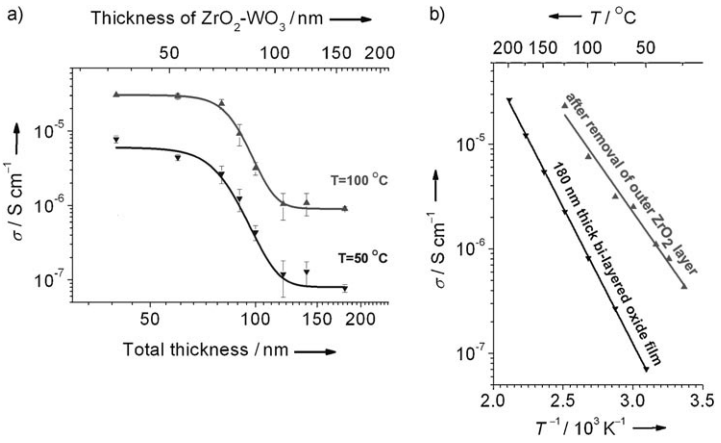

Figure 3. a) Proton conductivity as a function of film thickness for Zr–W/anodic oxide/Au in dry Ar atmosphere at 50 and 100 °C. b) Arrhenius plot of proton conductivity for 180 nm-thick anodic oxide film before and after dissolution of outer ZrO_2 layer in hydrofluoric acid.

effect of the outer ZrO_2 layer. Thickness-dependent conductivity was recently observed in amorphous oxide thin films. Berkemeier et al. reported that Li^+-ion conductivity in $0.2\,Li_2O/0.8\,B_2O_3$ glass films was exponentially enhanced by reduction of its thickness to less than 100 nm.[21] They explained this phenomenon by finite-size scaling in percolative conduction.[22] There are ion-conducting channels in the network of oxide glass. In the Li–B–O glass, the conducting channels consist of clusters of nonbridging oxygen (NBO) sites. The population of the NBO sites is below the percolation threshold; the NBO clusters accumulate inside the glass layer. If the thickness of the layer is in the range of the average size of the clusters, channels connecting the two electrodes are formed and increase the conductivity of the ionic layer. The number of channels connecting the two electrodes increases, and hence the conductivity increases with decreasing film thickness.

Similar size-scaling behavior was also observed for proton conduction in amorphous aluminosilica thin films prepared by a layer-by-layer sol–gel process.[23] The thickness dependence of proton conductivity followed a power law with a fixed index of −2.1, as predicted by the finite-scaling model of percolative conduction.[24] In the present amorphous anodic ZrO_2/WO_3 film, the dependence of proton conductivity on thickness does not follow a simple power law. This may be because the as-formed anodic film consists of two layers with an outer layer free of tungsten species. In addition, phosphate anions are present in the outer half of the film thickness. Such a layered structure may also influence the dependence of the proton conductivity on thickness. In one of our other experiments, we found that anodic ZrO_2 thin films formed on zirconium showed no detectable proton conductivity up to 200 °C. Thus, it is likely that the outer tungsten-free ZrO_2 layer in the anodic oxide film formed on Zr/50 at % W is more resistive for proton conduction than the inner ZrO_2/WO_3 layer. To examine the influence of the outer ZrO_2 layer on proton conductivity, it was chemically dissolved from the 180 nm-thick anodic oxide film in 1 wt % hydrofluoric acid. Atomic force microscopy (AFM) revealed that the surface of the anodic film was still flat after chemical dissolution, and the remaining film thickness was estimated by glow-discharge optical-emission spectroscopic depth profiling. The estimated thickness of the anodic oxide film after chemical dissolution was 158 nm; the reduction in film thickness was 12 %. Thus, only the outer ZrO_2 layer was dissolved. X-ray photoelectron spectroscopic (XPS) analysis of the film surface revealed that the cationic percentage of tungsten was 59 at %, which is in agreement with the composition of the inner layer determined by RBS (Supporting Information, Table S1).

The conductivity of the anodic film increased by almost one order of magnitude after removing the outer ZrO_2 layer (Figure 3b and Figure S2 in the Supporting Information). In addition, E_a decreased from 55 to 36 kJ mol^{-1} on dissolving the outer layer. This indicates that the thin outer ZrO_2 layer free from tungsten species has high resistivity for proton conduction. The E_a value for the thick film (158 nm) after dissolution of the outer ZrO_2 layer was still higher than that of the 40 nm-thick film (27 kJ mol^{-1}), in which a 4 nm-thick ZrO_2 layer was present at the oxide surface. The conductivity of the 158 nm-thick film without the outer ZrO_2 layer was also lower than that of the 40 nm-thick film with outer layer. The conductivity of the latter at 100 °C was approximately four times that of the former. This difference may increase after removing the outer ZrO_2 layer of the 40 nm-thick film. Thus, the size-scaling effect should also contribute to the proton conductivity of the present anodic ZrO_2/WO_3 films.

The presence of phosphate anions in the anodic ZrO_2/WO_3 film has little influence on proton conductivity. This was confirmed by forming phosphate-free anodic ZrO_2/WO_3 films in disodium molybdate electrolyte and measuring electrical resistivity by an ac impedance technique. In the molybdate electrolyte, electrolyte anions, that is, molybdenum species, were not incorporated into the anodic film.[1] In the anodic ZrO_2/WO_3 films formed in both electrolytes, similar proton conductivity was observed.

In summary, the present work demonstrates that an efficient proton-conducting ZrO_2/WO_3 film can be fabricated simply by anodizing Zr/W alloy. The enhancement in conductivity by reducing the film thickness is of significant scientific interest and also of practical importance for application of the films to solid oxide fuel cells and other electrochemical devices. The ASR value of 0.2 Ω cm^2, which is the minimum requirement for electrolyte in fuel cells, is achieved at a temperature as low as 100 °C for 60 nm-thick anodic ZrO_2/WO_3 films (Figure 2b). Efficient proton conductivity of this material is possibly associated with the strong Brønsted acidity of the oxide. Various double oxides with strong Brønsted acidity can be fabricated readily by a combination of alloy deposition by physical vapor deposition (PVD) and anodization of the deposited material; such oxides show high potential as efficient proton conductors. In this work, part of the deposited Zr/W alloy was retained beneath the anodic ZrO_2/WO_3 film. The alloy film can be replaced by another electrode material, suitable for the particular application, by chemically etching the alloy film and subsequently depositing the selected electrode material. It may be also possible to convert all the alloy film to anodic oxide by controlling the thickness of the deposited alloy film to remove the alloy film unsuitable for the application.

Amorphous WO_3-based double-oxide nanofilm is a new class of proton-conducting electrolyte. Understanding the precise mechanism of proton conduction requires detailed structural characterization, including identification of the presence of a conducting channel and its size. Such research is of significant importance for the development of materials with further improved conductivity. The present ZrO_2/WO_3 films should be the first example of efficient proton-conducting materials prepared by anodization. We expect that our present results will open up a new way for fabrication of next-generation proton-conductive materials.

Received: July 2, 2009
Published online: September 8, 2009

Keywords: amorphous materials · anodic oxidation · conducting materials · proton transport · thin films

[1] K. Shimizu, K. Kobayashi, G. E. Thompson, P. Skeldon, G. C. Wood, *Philos. Mag. B* **1996**, *73*, 461.

[2] a) K. Tsujii, T. Yamamoto, T. Onda, S. Shibuichi, *Angew. Chem.* **1997**, *109*, 1042; *Angew. Chem. Int. Ed. Engl.* **1997**, *36*, 1011; b) H. Habazaki, K. Shimizu, S. Nagata, K. Asami, K. Takayama, Y. Oda, P. Skeldon, G. E. Thompson, *Thin Solid Films* **2005**, *479*, 144; c) E. Balaur, J. M. Macak, L. Taveira, P. Schmuki, *Electrochem. Commun.* **2005**, *7*, 1066; d) C. A. Grimes, *J. Mater. Chem.* **2007**, *17*, 1451.

[3] T. Norby, *Solid State Ionics* **1999**, *125*, 1.

[4] a) K. Schmidt-Rohr, Q. Chen, *Nat. Mater.* **2008**, *7*, 75; b) O. Diat, G. Gebel, *Nat. Mater.* **2008**, *7*, 13.

[5] P. Heo, M. Nagao, M. Sano, T. Hibino, *J. Electrochem. Soc.* **2007**, *154*, B53.

[6] P. Heo, K. Ito, A. Tomita, T. Hibino, *Angew. Chem.* **2008**, *120*, 7959; *Angew. Chem. Int. Ed.* **2008**, *47*, 7841.

[7] a) S. M. Haile, D. A. Boysen, C. R. I. Chisholm, R. B. Merle, *Nature* **2001**, *410*, 910; b) D. A. Boysen, T. Uda, C. R. I. Chisholm, S. M. Haile, *Science* **2004**, *303*, 68.

[8] G. Busca, *Chem. Rev.* **2007**, *107*, 5366.

[9] a) H. Matsuhashi, H. Motoi, K. Arata, *Catal. Lett.* **1994**, *26*, 325; b) K. Arata, *Appl. Catal. A* **1996**, *146*, 3.

[10] B. C. H. Steele, A. Heinzel, *Nature* **2001**, *414*, 345.

[11] J. H. Shim, C. C. Chao, H. Huang, F. B. Prinz, *Chem. Mater.* **2007**, *19*, 3850.

[12] a) Y. Aoki, E. Muto, A. Nakao, T. Kunitake, *Adv. Mater.* **2008**, *20*, 4387; b) Y. Aoki, E. Muto, S. Onoue, N. Aiko, T. Kunitake, *Chem. Commun.* **2007**, 2396.

[13] Y. Z. Li, T. Kunitake, Y. Aoki, E. Muto, *Adv. Mater.* **2008**, *20*, 2398.

[14] L. Iglesias-Rubianes, P. Skeldon, G. E. Thompson, U. Kreissig, D. Grambole, H. Habazaki, K. Shimizu, *Thin Solid Films* **2003**, *424*, 201.

[15] H. Habazaki, T. Matsuo, H. Konno, K. Shimizu, S. Nagata, K. Matsumoto, K. Takayama, Y. Oda, P. Skeldon, G. E. Thompson, *Electrochim. Acta* **2003**, *48*, 3519.

[16] Q. Lu, S. Mato, P. Skeldon, G. E. Thompson, D. Masheder, H. Habazaki, K. Shimizu, *Electrochim. Acta* **2002**, *47*, 2761.

[17] J. T. S. Irvine, D. C. Sinclair, A. R. West, *Adv. Mater.* **1990**, *2*, 132.

[18] A. S. Nowick, A. V. Vaysleyb, *Solid State Ionics* **1997**, *97*, 17.

[19] N. Bonanos, *Solid State Ionics* **1992**, *53*, 967.

[20] M. Nagao, T. Kamiya, P. Heo, A. Tomita, T. Hibino, M. Sano, *J. Electrochem. Soc.* **2006**, *153*, A1604.

[21] F. Berkemeier, M. S. Abouzari, G. Schmitz, *Appl. Phys. Lett.* **2007**, *90*, 113110.

[22] F. Berkemeier, M. R. S. Abouzari, G. Schmitz, *Phys. Rev. B* **2007**, *76*, 024205.

[23] Y. Aoki, H. Habazaki, T. Kunitake, *Electrochem. Solid-State Lett.* **2008**, *11*, P13.

[24] D. Stauffer, A. Aharony, *Introduction to Percolation Theory*, CRC Press, Boca Raton, FL, **1991**.

